

Transmission Target for a MEMS X-Ray Source

Paweł Urbański¹, Marcin Białas, Michał Krysztof¹, and Tomasz Grzebyk¹

Abstract—This paper describes a major step towards the development of the first fully MEMS X-ray source. It focuses mostly on the development of a transmission target that is responsible for converting the electron beam into radiation. The simulation and experimental results are presented, allowing investigation of the influence of the target material, target thickness, and electron beam energy on the obtained X-ray radiation intensities and spectra. It has been proven that one can apply a silicon membrane as an X-ray target working with energies below 25 keV. It has also been shown that covering the membrane with metals such as nickel or tantalum can significantly improve the radiation intensity. Moreover, the article presents how exactly these metals contribute to radiation spectrum, i.e. which gives more coherent beam and which broadband. [2023-0040]

Index Terms—MEMS, X-ray source X-ray target, X-ray radiation.

I. INTRODUCTION

X-RAY inspection has been applied in many different areas for more than a century: in medicine, metallurgy, crystallography, electronics, or environmental science [1], [2], [3], [4], [5]. However, many research groups are still active in this field. There are few visible trends present in the literature related to: miniaturization, exploration of new functionalities, and new applications [6], [7], [8], [9], [10], [11], [12], [13]. The first aspect is the most important since it allows for the investigation of two others. Having a miniature X-ray source, one can think of developing low-cost X-ray tomography instruments, inspection of very small, e.g., biological objects, etc. MEMS technology seems to be very promising for the production of miniature X-ray sources. Despite the fact that it is often applied to prepare some elements of the X-ray source, until now there has been no X-ray source fabricated completely in MEMS technology. Few problems must be overcome to achieve this goal. Such a source requires an efficient electron emitter [7], [8], [9], [12], [13], a proper target to convert the accelerated electrons into radiation, stable, high-vacuum conditions [14], [15], [16], and in the case of high intensity source – a cooling systems [17].

Classical X-ray sources usually contain a thermal cathode, a copper or tungsten target, and are sealed in a hermetic glass

Manuscript received 15 March 2023; revised 25 May 2023; accepted 4 June 2023. Date of publication 19 June 2023; date of current version 2 August 2023. This work was supported by the Polish National Science Centre under Project 2021/41/B/ST7/01615. Subject Editor T. Tsuchiya. (Corresponding author: Tomasz Grzebyk.)

The authors are with the Faculty of Electronics, Photonics and Microsystems, Wrocław University of Science and Technology, 50-372 Wrocław, Poland (e-mail: tomasz.grzebyk@pwr.edu.pl).

Color versions of one or more figures in this article are available at <https://doi.org/10.1109/JMEMS.2023.3283536>.

Digital Object Identifier 10.1109/JMEMS.2023.3283536

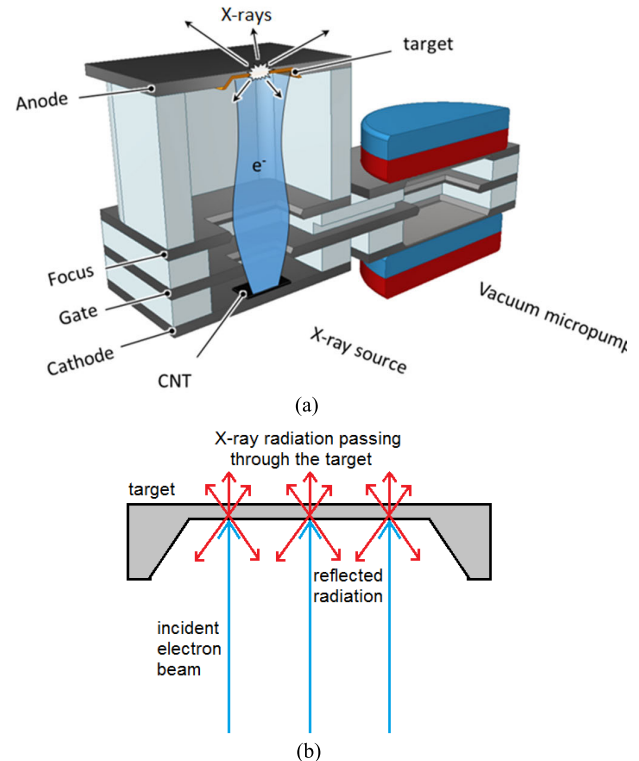


Fig. 1. Scheme of the MEMS X-ray source (a) and illustration of the electron-radiation conversion (b).

or ceramic tube. In most cases, they work in a reflective mode: the electron beam collides with a tilted target, and the generated X-ray radiation leaves the housing through a beryllium window on its side wall. Although such an approach is advantageous in many situations (operation under high power, protection of an electron source from scattered X-rays), it cannot be transferred directly to MEMS, which usually has a form of a silicon-glass multilayer structure.

We propose a different approach. In our concept, the completely MEMS X-ray source will consist of an electron gun formed of a field-emission cathode (CNT or silicon tip), silicon gate and focus electrodes, proper glass spacers, and an MEMS ion-sorption vacuum pump attached to a side, responsible for providing high vacuum conditions [18], [19], [20]. The X-ray source will work in transmission mode. X-rays generated at the target in the form of a membrane will leave the source through the top layer (Fig. 1). Reflected X-rays will be absorbed by silicon and glass elements.

The target is the most important element of the X-ray source responsible for the conversion of the electron beam to radiation. X-ray radiation is formed when a high-energy electron beam collides with a target material (Fig. 2a). During

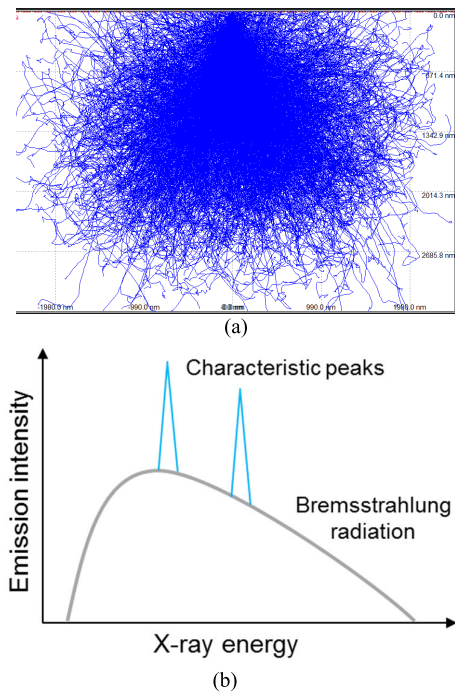


Fig. 2. Scattering of the electron beam in the target; from CASINO software (a) and an example of the X-ray spectrum (b).

that process, electrons lose their kinetic energy because of interactions with atoms of the target in the form of elastic scattering (e.g., trajectory change) or inelastic scattering (e.g., ionization collisions). The first process leads to the formation of a hump on the emission spectrum (so-called Bremsstrahlung (BS) radiation), and the second is responsible for the presence of the characteristic peaks (Fig. 2b). It must also be underlined that not more than 1% of electron energy is transferred to radiation, the rest is wasted as heat.

The choice of a certain target material, its thickness, and shape affect the intensity and quality (spectral and spatial distribution) of the emitted X-ray beam, as well as the heat dissipation. On the basis of the simulation and measurement results, the authors tried to investigate the relations between the mentioned parameters and optimize them.

The plan was to use the source as a relatively low-energy instrument (5-25 keV). This is a range not common for most X-ray sources, and thus many initial tests had to be performed.

II. METHODS

The simulations were performed with CASINO and Win X-ray software [21], [22]. Both programs use the Monte Carlo method for calculating electron trajectories in solid materials. The CASINO program focuses on simulating the effects happening to the electron beam in the scanning electron microscope. The Win X-ray program is its extension, which provides complete simulation of the X-ray spectrum.

Each time, 2000 electrons were used for the calculations. Simulations allowed to show how the electrons are scattered in the material, where exactly they lose energy, and how deep they can reach. Due to that, it was possible to obtain emission spectra for different materials and electron beam energies.

It must be taken into account that the targets working in the transmission mode do not only generate radiation, but can also absorb part of it – this effect was also calculated.

Experimental results were obtained using a well-defined electron beam from a scanning electron microscope (operating in almost static mode, beam size 50 nm, 1 nA) and a beam generated from a thermal cathode (2 mm spot size, 100 μ A). Signals were recorded on a CMOS matrix placed behind the (Cd,Zn)S:Ag or CsI(Tl) scintillators, which gave the highest optical signals for the low-energy X-ray beam.

To determine the emission spectra, the Ketek AXAS-D spectrometer was utilized.

III. RESULTS

A. Silicon Target

The first aspect that was investigated was the possibility of using silicon as the target material. It is the material used for the preparation of all other electrodes of the X-ray source, and thus, from a technological point of view, it was the easiest choice. It is possible to form a membrane with a desired size and thickness by photolithography and KOH etching processes and connect it to a glass spacer by anodic bonding. The use of silicon as a target material also allows the integration of the X-ray source with another microsystem or μ TAS. One can add, for example, a microfluidic channel for an analyzed sample right above the membrane, or with water, around the membrane – for cooling.

However, silicon is not a typical material applied in X-ray sources (neither for X-ray generation nor for its transmission). Silicon is a relatively low mass material, and the mass number is one of the most important parameters in terms of the generation and absorption of X-ray radiation. It will not generate as much radiation as heavier materials, and will not allow to pass through as much radiation as, e.g. beryllium window.

To explore this aspect, first computer simulations were performed. They showed that the Si target generates a lot of radiation, but most of the energy is concentrated in a 1.74 keV peak and that the Bremsstrahlung hump is relatively low (Fig. 3). The presence of a characteristic peak below 2 keV and a low hump, especially for the higher energy range, can be problematic for further application for two different reasons. First, low-energy radiation (<5keV) is highly absorbed by most materials. Second, the majority of detectors are designed to cooperate with commercial X-ray tubes, working usually above 50 keV. Thus, it was not guaranteed that any image can be obtained from this signal.

The spectral measurements showed almost identical results predicted by the simulations (Fig. 4).

More important were the results obtained on a scintillator screen. Despite the mentioned concerns, the X-ray image was clearly visible (Fig. 5a). It had a Gaussian-like distribution (Fig. 5b) - it was the most intensive in the central part of the screen and vanishes at the edges – which is characteristic for conically emitted X-ray beams. Of course, the radiation is generated in all directions, but mostly the part that is close to the axis can leave the source.

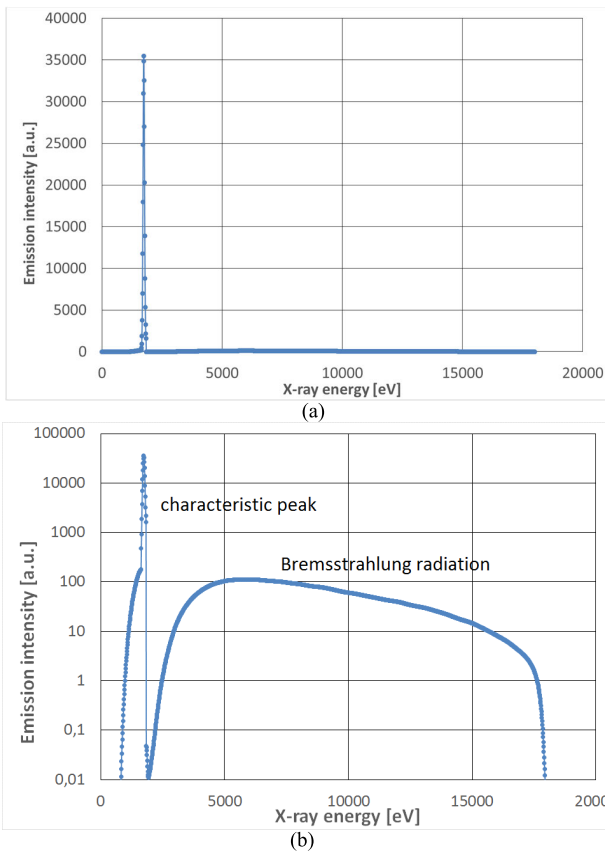


Fig. 3. Simulated X-ray spectrum of Si (Win X-ray software): a) in linear scale, b) in logarithmic scale.

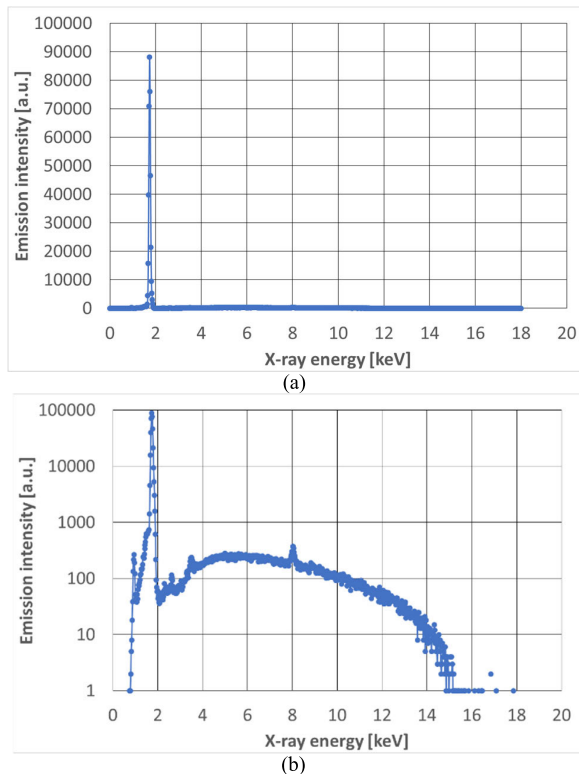
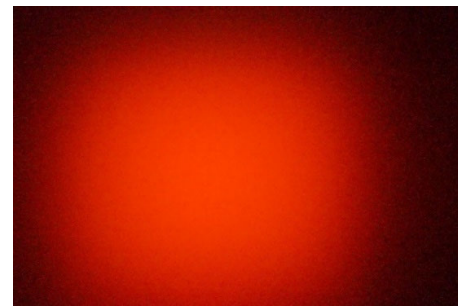
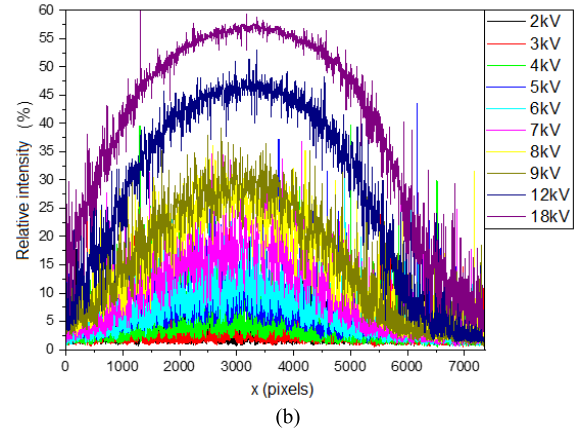


Fig. 4. Measured X-ray spectrum of Si: a) in linear scale, b) in logarithmic scale.

The intensity of the X-ray beam changed with the incident electron energy (Fig. 6). Below 6 keV, it was almost at the



(a)



(b)

Fig. 5. Signal recorded on a CCD screen with a silicon target, $E = 18 \text{ keV}$, Si thickness = $15 \mu\text{m}$ (a), and the cross-section of the beam for different X-ray energies.

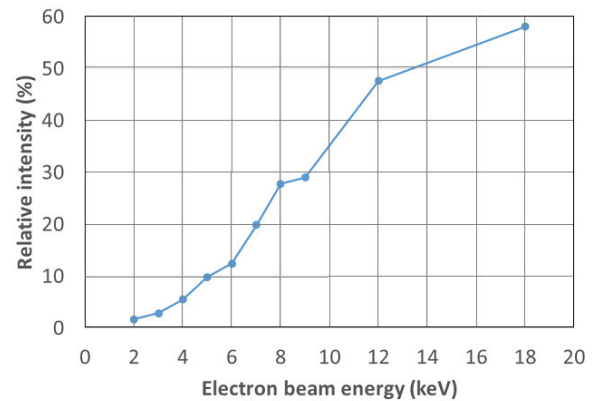


Fig. 6. Intensity of the image as a function of energy.

noise level (the image intensity was below 10%, expressed in a relative gray scale). Between 6 and 12 keV, the intensity increased from 10 to 50%. This level was high enough to obtain clearly visible images. A further increase of the electron energy increased the intensity of the X-ray signal, but not at the same rate as before.

Simulations and measurements indicated that the electron energy also significantly affects the X-ray spectra (Fig. 7). The high voltage applied to the target increases the intensity of a continuous spectrum and the height of the characteristic peak, even by a few orders of magnitude. The edge of the Bremsstrahlung hump shifts right (to higher energies), but majority of X-ray photons have energies around 4-6 keV, independently on the electron energy.

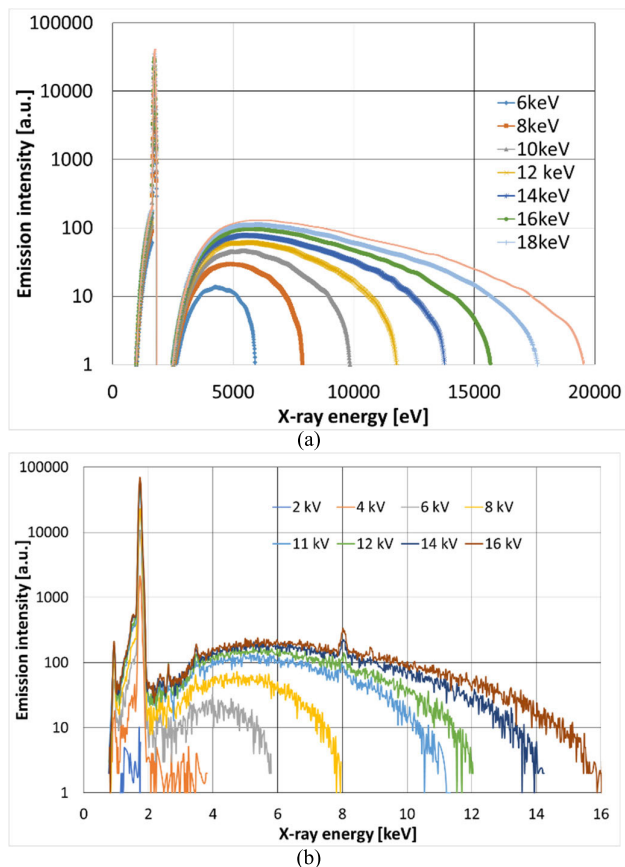


Fig. 7. Spectrum of emission for different electron beam energies: a) simulation results (Win X-ray), b) experiment.

Operation in transmission mode required investigation of one more aspect. The target in that case not only allows for the generation of X-ray photons but can also absorb part of them before they reach the sample. Thus, it should be thick enough to allow all electrons to decelerate but not too thick not to absorb the generated radiation. Therefore, the choice of the optimal thickness is an essential task.

The Monte Carlo simulation shows that the depth of electron penetration depends mostly on the electron energy. For silicon target and electron energy lower than 25 keV, all electrons lose their kinetic energy in 7- μm thick layer. The majority (90%) of the X-ray radiation is generated in the first 4 μm of material (Fig. 8). Thus, taking only this fact into account, the silicon membrane that forms the target does not have to be thicker than a few micrometers.

If the membranes are too thick, they reduce the transmission of the signal (Fig. 9). However, it refers mostly to low-energy radiation, especially if the thickness does not exceed 15-30 μm . This means that a proper silicon target does not cause high attenuation of a signal in the range useful for X-ray examination. Thus, the use of silicon as a target should not worsen the X-ray images in comparison to sources with classical beryllium windows.

It might be interesting that there is also a second transmission window near 2 keV for low-thickness membranes, but it is useless in the case of future X-ray applications.

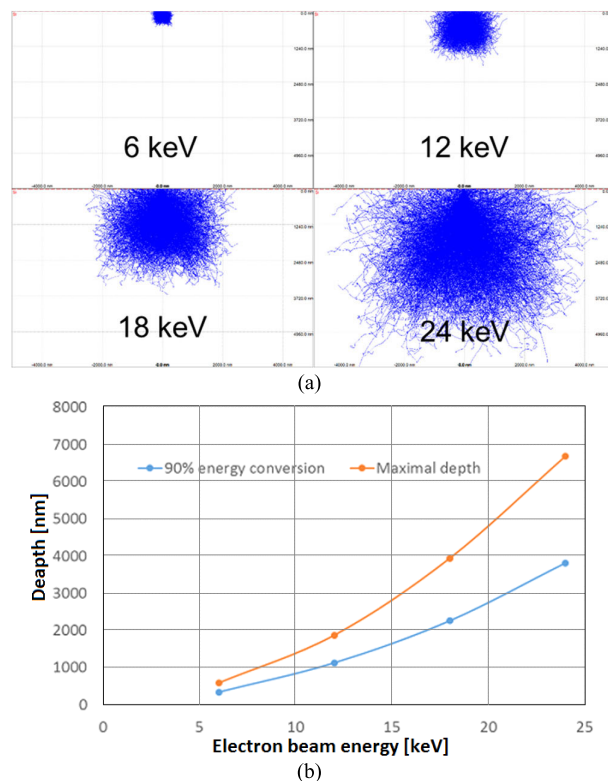


Fig. 8. Simulation results using CASINO software of a penetration depth of electrons: a) electron trajectories in Si target, b) penetration depth as a function of electron energy.

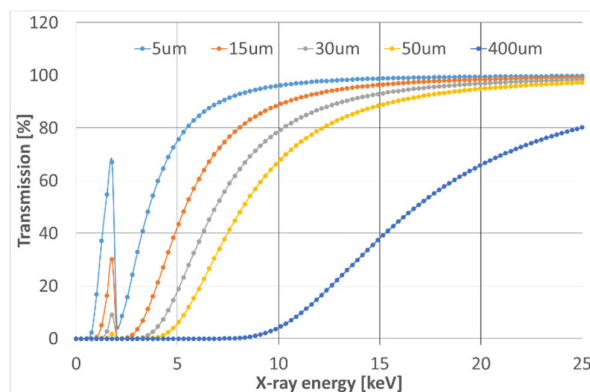


Fig. 9. Transmission of X-ray radiation through the membrane.

Measurements performed for structures with a thickness from 10 to 400 μm also revealed that the thinner the membrane, the more intensive signal that comes to the detector (Fig. 10). For technical reasons (possibility of mechanical damage and heat dissipation), the optimal value was chosen as 15 μm . For such membranes, the authors did not observe any thermal damage, even during high-current operation (300 μA , 25 keV, several minutes of continuous work).

The absorption of low-energy photons, which it may cause, might even be advantageous because the transmitted signal can be more monochromatic. Furthermore, when one looks at the 400 μm -thick target, one can see that it absorbs more than 99% of all radiation. This fact is also positive because if the target is formed as a membrane, which is thinned only in

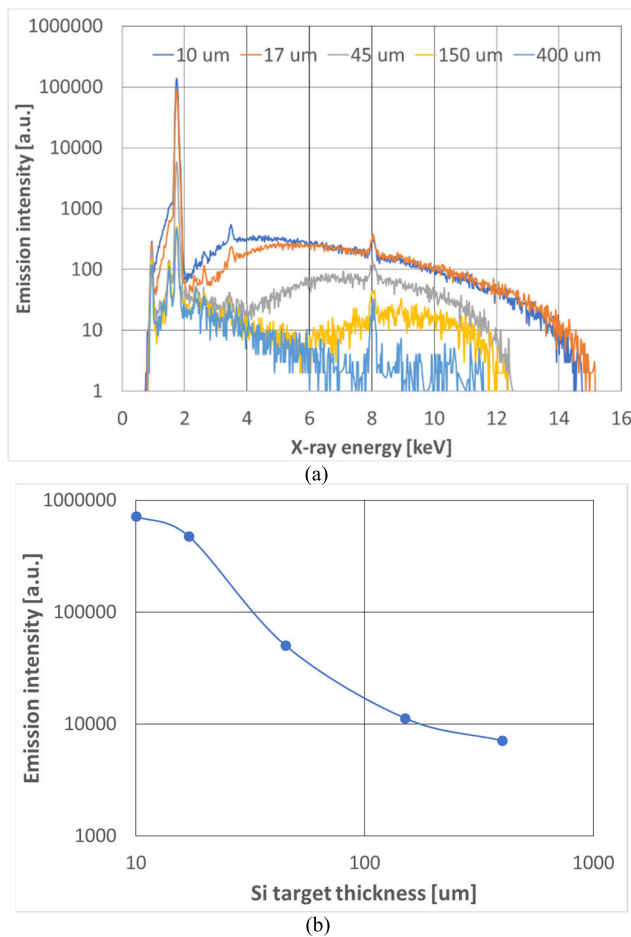


Fig. 10. Effect of membrane thickness on: a) recorded spectra, b) X-ray emission intensity.

the central part of the silicon chip and the rest of it is thick, the signal will come only through a small spot, and the user sitting on the side will be protected. Moreover, the beam will be more conical.

B. Covering Materials

The experiments presented so far indicated that silicon can serve as a target material. However, it has also been investigated whether one can increase the intensity of the signal by covering the target with different materials. Conventional sources usually use copper, molybdenum, tungsten or gold targets. The scope of materials for a low-energy (<25 keV), MEMS target was narrowed mainly to those that are often used in microengineering technology. Taking different aspects into account: atomic mass, energy of characteristic peaks, layer adhesion, temperature of oxidation, price, and availability, two layers have been chosen for further analysis and comparison with silicon – nickel and tantalum.

Simulations showed (Fig. 11) that the heavier the element, the more intensive the Bremsstrahlung radiation. This is a fact often mentioned in the literature [13]. However, the relation between the mass and the intensity of the characteristic peaks is not that straightforward. Light elements such as Si have characteristic peaks below 2 keV; thus, they will not contribute much to the useful transmitted signal. Medium-weight atoms

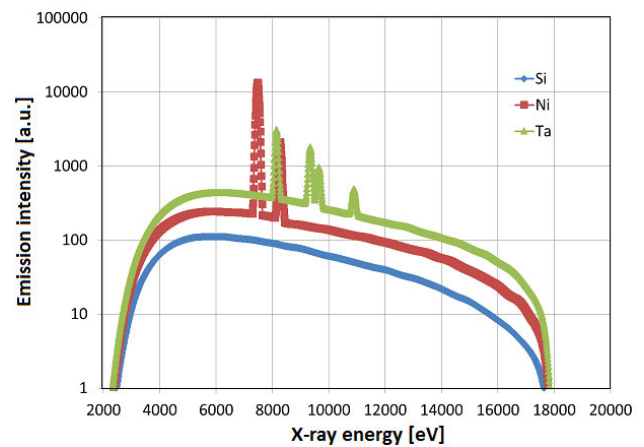


Fig. 11. Simulated emission intensity of silicon targets covered with different materials (Win X-ray software).

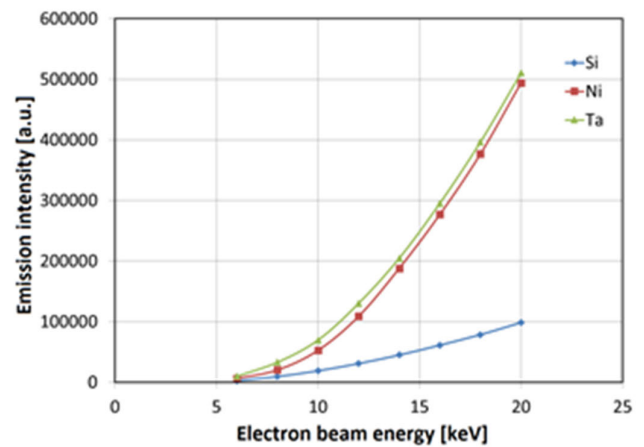
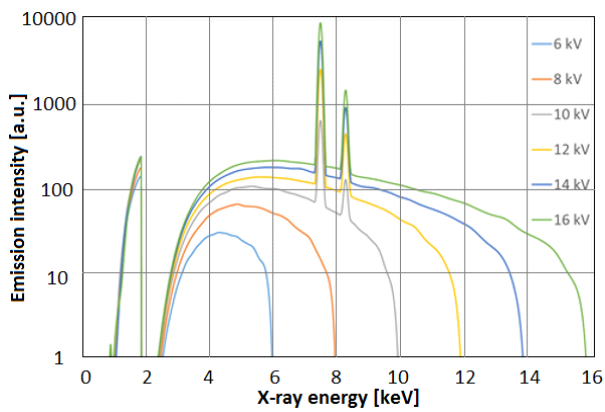


Fig. 12. Simulated results of the intensity of emitted X-rays as a function of electron beam energy (Win X-ray software).

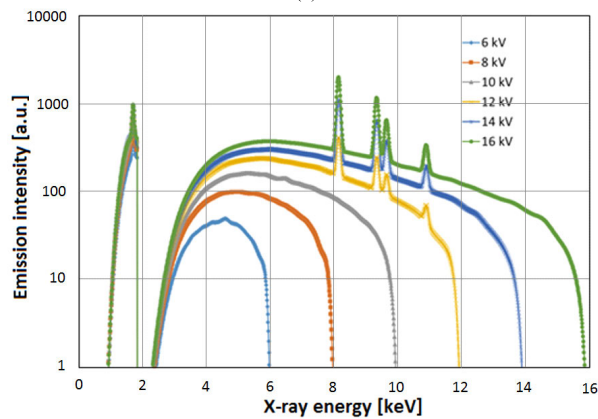
(such as Ni, Cu) have characteristic K-line peaks near 10 keV. Heavy atoms (like Ta, W, Au) have K-line peaks above 50 keV, but L-line peaks also near 10 keV. This is the preferred range when the source is operated below 25 kV - the energy of the peaks is close to the maximum of the continuous spectrum, which makes the beam more coherent. However, L-line peaks are never as intensive as those of the K-line.

The total X-ray intensity depends on the acceleration voltage. Simulations show that for all three materials, it increases rapidly above 6 kV (Fig. 12). It is clearly visible that although silicon can be used as an emissive material, other coverings, such as Ni and Ta, give much stronger signals (up to 5 times).

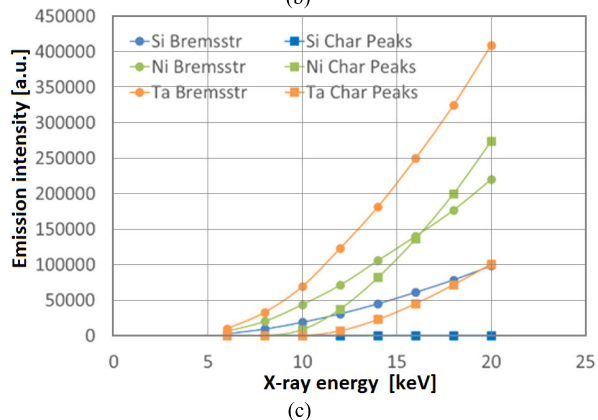
As can be noticed, the overall emission is similar in the case of both coverings, but deeper analysis of the spectra reveals some interesting nuances. First, a fairly obvious fact is that to observe any peaks, the acceleration voltage needs to be higher than their energy. In the case of nickel, 10 kV is sufficient to see both emission peaks (Fig. 13a), but for tantalum, 12 kV must be applied, and even then, the height of the peaks is very low (Fig. 13b). This is because for nickel K-line peaks are visible, for tantalum – not-so-intensive L-line peaks. With increasing voltage, the energy concentrated in the



(a)



(b)

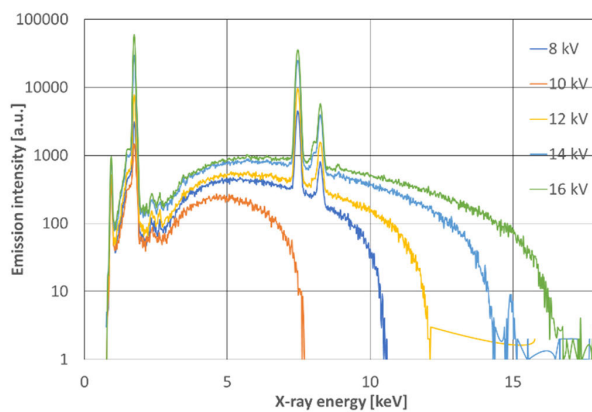


(c)

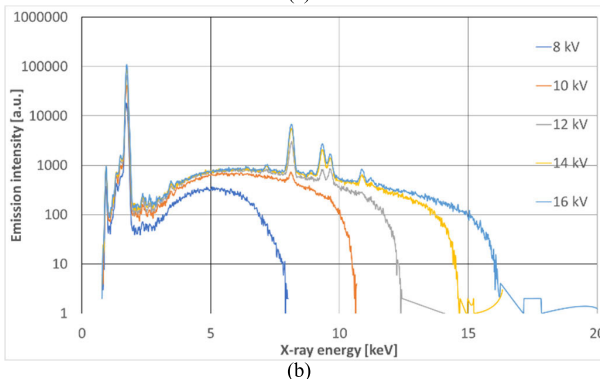
Fig. 13. Simulation results of the influence of the acceleration voltage on the X-ray emission (Win X-ray software): a) spectra for nickel, b) spectra for tantalum, c) comparison of emission intensity for Ni, Ta, and Si.

peaks increases, however the rate in which it happens is much more pronounced for nickel than for tantalum. At 16 keV it even exceeds the energy cumulated in the whole BS hump. For comparison, the energy of tantalum peaks is almost negligible with respect to BS (Fig. 13c). Thus, the fact that the characteristics presenting total emission intensity overlap is rather a coincidence, since they take the origin in summing up two phenomena, which are completely different for Ni and Ta.

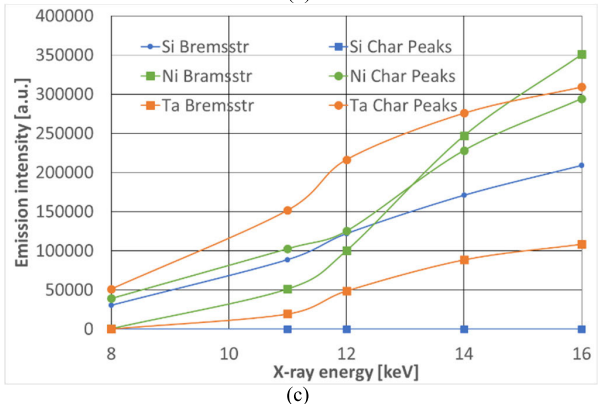
The simulation results have been confirmed in the spectrometric measurements (Fig. 14). The same conclusion can be drawn from the experiments. However, there is one fact that is different in both situations – it is the behavior of the emission intensity characteristics in the high energy range. Instead of a continuous increase, one can notice a saturation. This fact



(a)



(b)



(c)

Fig. 14. Spectrometric results of the influence of the acceleration voltage on the X-ray emission: a) spectra for nickel, b) spectra for tantalum, c) comparison of emission intensity for Ni, Ta, and Si.

can be easily explained, when one takes into account that the simulations were carried out for an ideal case, in which all radiation is generated within a metal layer.

In reality, when silicon is covered with a thin metal layer, some electrons can pass through the metal and generate less intense radiation in silicon. The last effect is mostly dominant when the electron energy is high, and this is clearly illustrated in the curves.

The effect of metal covering has also been investigated by measuring the intensity of the signal coming from the irradiated scintillator screen (Fig. 15). The differences between materials are not as significant as in the simulations, but the screen placed behind the silicon target is clearly darker than those for the other two materials. One can also see that the use of Ta or Ni coverings can reduce the voltage necessary to obtain an intensive light signal by 2-4 kV.

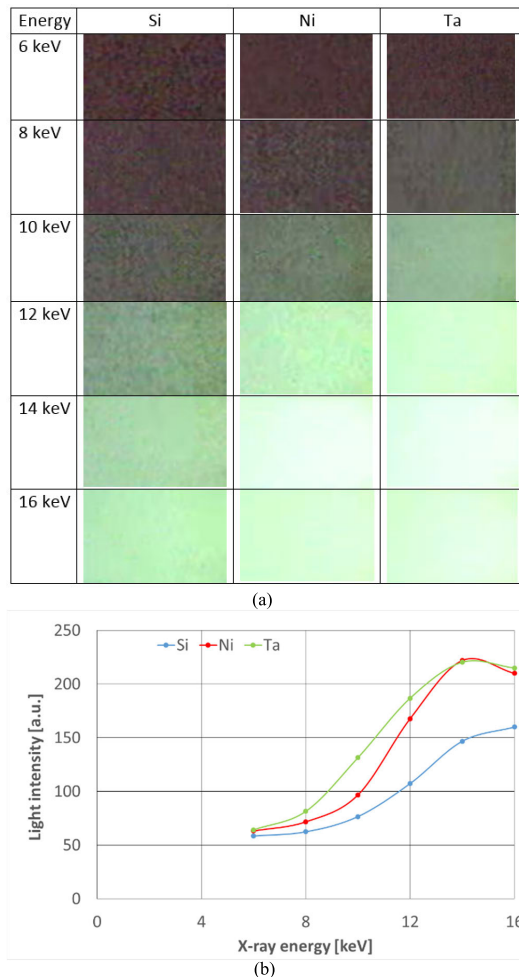


Fig. 15. X-ray screen illuminated by radiation coming from silicon, nickel, and tantalum targets (a), and the intensity measured for different electron energies (b).

IV. CONCLUSION

This article presented how to fabricate an X-ray source using MEMS technology. The simulation and experimental results concentrated on one of the most important elements of such a source, the target that converts an accelerated electron beam to radiation. It has been shown that intensive radiation can be generated using a 15- μm -thick silicon target working in a transmission mode; however, targets covered with an additional layer of nickel or tantalum can increase the intensity of the obtained signals by a few times or decrease the voltage necessary to obtain them by 2–4 kV. Comparison of Ta and Ni leads to the conclusion that in the case of total emission energy, it does not matter which one is chosen, but nickel will emit a more monochromatic signal, because more energy is concentrated in the characteristic peaks and in the case of Ta in Bremsstrahlung.

The choice of a proper X-ray target is one of the most important tasks in the construction of a MEMS X-ray source. However, to fabricate a complete device several other aspects still need to be investigated. A proper, stable field emission source has to be chosen, the whole structure must be hermetically sealed, and the applied micropump should be able to maintain high vacuum conditions during the device operation. All these factors will determine the total lifetime of the whole instrument. Currently, it is hard to predict. However, initial

measurements suggest that the stability and lifetime of a field emitter would be the most important issue. Other aspects like vacuum maintenance and robustness of the membrane have been initially investigated and do not seem to be problematic.

REFERENCES

- [1] J. Kirz, C. Jacobsen, and M. Howells, "Soft X-ray microscopes and their biological applications," *Quart. Rev. Biophys.*, vol. 28, no. 1, pp. 33–130, 1995.
- [2] T. J. Bowser, S. K. Mathanker, and P. R. Weckler, "X-ray applications in food and agriculture: A review," *Trans. ASABE*, vol. 56, no. 3, pp. 1227–1239, May 2013.
- [3] A. A. Bunaciu, E. G. Udriștiou, and H. Y. Aboul-Enein, "X-ray diffraction: Instrumentation and applications," *Crit. Rev. Anal. Chem.*, vol. 45, no. 4, pp. 289–299, 2015.
- [4] F. Mees, R. Swennen, M. V. Geet, and P. Jacobs, "Applications of X-ray computed tomography in the geosciences," *Geolog. Soc., London, Special Publications*, vol. 215, pp. 1–6, Jan. 2003.
- [5] E. R. Davies, "Visual inspection, automatic (robotics)," in *Encyclopedia of Physical Science and Technology*, 3rd ed. San Diego, CA, USA: Academic, 2003, pp. 489–508.
- [6] A. Górecka-Drzazga, "Miniature X-ray sources," *J. Microelectromech. Syst.*, vol. 26, no. 1, pp. 295–302, 2017.
- [7] S. Cheng, F. A. Hill, E. V. Heubel, and L. F. Velásquez-García, "Low-bremsstrahlung X-ray source using a low-voltage high-current-density nanostructured field emission cathode and a transmission anode for markerless soft tissue imaging," *J. Microelectromech. Syst.*, vol. 24, no. 2, pp. 373–383, Apr. 2015.
- [8] C. Puett et al., "An update on carbon nanotube-enabled X-ray sources for biomedical imaging," *Wiley Interdiscipl. Rev., Nanomed. Nanobiotechnol.*, vol. 10, no. 1, 2018, Art. no. e1475.
- [9] J.-W. Jeong, J.-W. Kim, J.-T. Kang, S. Choi, S. Ahn, and Y.-H. Song, "A vacuum-sealed compact X-ray tube based on focused carbon nanotube field-emission electrons," *Nanotechnology*, vol. 24, no. 8, 2013, Art. no. 085201.
- [10] S. Cornaby et al., "Simultaneous XRD/XRF with low-power X-ray tubes," *Adv. X-Ray Anal.*, vol. 45, pp. 34–40, Jan. 2002.
- [11] R. Behling, *Modern Diagnostic X-Ray Sources, Technology, Manufacturing, Reliability*. Boca Raton, FL, USA: CRC Press, 2015.
- [12] A. Basu, M. E. Swanwick, A. A. Fomani, and L. F. Velásquez-García, "A portable X-ray source with a nanostructured Pt-coated silicon field emission cathode for absorption imaging of low-Z materials," *J. Phys. D, Appl. Phys.*, vol. 48, no. 22, Jun. 2015, Art. no. 225501.
- [13] B. Diop and V. T. Binh, "Quasi-monochromatic field-emission X-ray source," *Rev. Sci. Instrum.*, vol. 83, Sep. 2012, Art. no. 094704.
- [14] T. Grzebyk, "MEMS vacuum pumps," *J. Microelectromech. Syst.*, vol. 26, no. 4, pp. 705–717, Aug. 2017.
- [15] A. Basu and L. F. Velásquez-García, "An electrostatic ion pump with nanostructured Si field emission electron source and Ti particle collectors for supporting an ultra-high vacuum in miniaturized atom interferometry systems," *J. Micromech. Microeng.*, vol. 26, no. 12, Dec. 2016, Art. no. 124003.
- [16] S. R. Green, R. Malhotra, and Y. B. Gianchandani, "Sub-torr chip-scale sputter-ion pump based on a Penning cell array architecture," *J. Microelectromech. Syst.*, vol. 22, no. 2, pp. 309–317, Apr. 2013.
- [17] J. Winter et al., "Heat management of a compact X-ray source for microbeam radiotherapy and FLASH treatments," *Med. Phys.*, vol. 49, no. 5, pp. 3375–3388, May 2022.
- [18] P. Urbanski, M. Bialas, M. Krysztof, and T. Grzebyk, "MEMS X-ray source: Electron-radiation conversion," in *Proc. 21st Int. Conf. Micro Nanotechnol. Power Gener. Energy Convers. Appl. (PowerMEMS)*, Dec. 2022, pp. 42–45.
- [19] M. Krysztof, P. Urbanski, T. Grzebyk, M. Hausladen, and R. Schreiner, "MEMS X-ray source: Electron emitter development," in *Proc. 21st Int. Conf. Micro Nanotechnol. Power Gener. Energy Convers. Appl. (PowerMEMS)*, Dec. 2022, pp. 248–251.
- [20] T. Grzebyk, P. Knapkiewicz, P. Szyszka, A. Gorecka-Drzazga, and J. A. Dziuban, "MEMS ion-sorption high vacuum pump," *J. Phys., Conf.*, vol. 773, Nov. 2016, Art. no. 012047.
- [21] P. Hovington, D. Drouin, and R. Gauvin, "CASINO: A new Monte Carlo code in C language for electron beam interaction—Part I: Description of the program," *Scanning*, vol. 19, pp. 1–14, Jan. 1997.
- [22] R. Gauvin, E. Lifshin, H. Demers, P. Horny, and H. Campbell, "Win X-ray: A new Monte Carlo program that computes X-ray spectra obtained with a scanning electron microscope," *Microsc. Microanal.*, vol. 12, pp. 49–64, Feb. 2006.